Academic Journal of Science and Technology
ISSN: 2771-3032 | Vol. 11, No. 2, 2024

Analysis of the Utility Tunnel Joint's Stress Characteristics Under Well Point Precipitation Conditions

Ben Li, Xinsheng Zhang

School of Civil Engineering, Central South University of Forestry and Technology, Changsha 410004, China

Abstract: The method by which groundwater influences subsurface buildings is relatively complex in the groundwater-rich regions of southern China. Notably, it substantially affects the pipe corridor junctions, which are crucial to impermeability. In order to analyze the forces on the utility tunnel joints during well-point precipitation, numerical modeling of the utility tunnel joints using the well-point precipitation method based on Finite element software was carried out, and a precipitation model tank was made to verify the model parameters and boundary restrictions. The results indicate that under well-point precipitation, the force variation of the bottom plate is more significant than that of the top plate at the same port and that in the joint section close to the precipitation point, the force variation of the bottom plate can reach 2-3 times that of the top plate. The spigot joint's bottom plate has a maximum tensile stress of 319.52 kPa, which raises the possibility of tensile damage. The well-point dewatering method has a higher likelihood of bottom plate cracks, which makes it a critical component to be watched during construction and operation.

Keywords: Utility Tunnel; Wall Point Precipitation; Groundwater Level; Finite Element Model.

1. Introduction

In recent years urban development, Underground utility tunnels have received much attention because of their numerous benefits, including saving ground area, reducing traffic congestion, and beautifying the city [1–4]. A utility tunnel is a typical underground structure that is highly vulnerable to the effects of groundwater buoyancy. Different water level distributions around the pipe corridor bring different lifting effects so that the pipe corridor experiences uneven forces, resulting in misalignment of the pipe corridor and the destruction of the overall stability of the structure of the pipe corridor. The joints are more likely to seepage and other safety issues. The “Technical code for urban utility tunnel engineering” GB 50838-2015) states that the interfacial stress of the elastic gasket at the waterproof joints of the pipe corridor shall be more than 1.5 MPa to meet the sealing and waterproofing requirements. In response to groundwater, the properties of the soil change simultaneously. That demonstrates the significance of researching how groundwater affects underground construction.

Currently, research is being done on how groundwater affects buildings. An YL[5] conducted an analysis of the impact of water on the tunnel face and perimeter pressure and came to the conclusion that the range of influence of negative pore water pressure increased with decreasing water level. An accurate numerical model for two-dimensional groundwater flow in aquifers was created by Encarnación Martnez-Moreno[6] to study the groundwater flow process near underground constructions. P. Gattinoni[7] examined the harm done to existing underground structures by groundwater during the regional rise of the groundwater table and concluded that the protection of underground structures should be achieved through the coordinated action of multiple schemes. E. Vasilyeva et al.[8] examined the processes by which groundwater retaining structures were damaged in different regions and offered improved procedures and actions to address the flaws of the structures and lessen the harm groundwater was causing. Regarding the effects of changing water levels. M. S. Aswathy[9] investigated the example of surface settlement of deep foundations in the Gangetic Plain and demonstrated that it was caused by dewatering following the installation of a collection chamber using the well sinking method. Soft soil and a high water table led the earth to slide toward the collection chamber, which produced severe settlement problems. In-depth research by Xu Guangli et al.[10] into the potential damage brought on by a rise in groundwater level led to the conclusion that the long-term change in groundwater level during operation should be considered. According to Wen Jie Song et al.'s [11] mechanical modeling study of the force behavior of subway station structures under various water levels, different groundwater levels cause significant vertical displacements and plastic changes in the soil nearby and a significant increase in the groundwater level nearby causes the overall deformation and flotation of the underground structure. J. Mamaghanian et al. [12] used four seepage models for groundwater rise to simulate the impact of groundwater on the performance of various earth retaining walls. By examining the model's stress, strain, and deformation, Maimunah et al. [13] evaluated the impact of reservoir level variation on the stability of an earth and rock dam model.

Numerous studies are now being conducted to examine the effects of the groundwater table on construction. Although the joints' stress is crucial for waterproofing, little is known about how pipe corridor joints respond to precipitation. It is essential to comprehend these stressful factors for waterproof pipe corridors. It is advantageous to safeguard the pipe corridor structure and explore the force deformation of pipe corridor joints under water level change using logical waterproofing methods. Using finite element analysis software, the author examined the stress characteristics of the integrated pipe corridor's joints under well-point precipitation conditions to give references for the pipe corridor's design,

construction, operation, and maintenance in the future. Drawing on this, the author created multiple scenarios with varying precipitation levels and carefully examined the stress-strain relationship of the joints as the water table fluctuated.

2. Modeling and Calculation

2.1. Precipitation Setup

It was determined how soil settling caused by the well-point precipitation method affected the force of underground pipe corridors. To replicate the different precipitation depths, an idealized model is constructed with a single homogeneous layer of soil, pumping well precipitation prior to construction, and the pumping well depth as the main control variable. Refer to Table 1 for working condition criteria. The pipe corridor is three meters below the surface and 3.2 meters high. The bottom of the pipe corridor and the bottom of the precipitation well are level at 6.2 meters below the surface of the precipitation.

Table 1. Precipitation simulation conditions

Number of pumping wells/pc	Pumping well depth/m	Working condition code
0		P0-W0
1	6.2	P1-W1
	10	P1-W2
	15	P1-W3
	20	P1-W4
	25	P1-W5

It is possible to determine the effect caused by a change in the precipitation depth by comparing the simulation results with those of the situation without precipitation (P0-W0).

2.2. Model Parameter Setting

The soil model material is clay, and the M-C model is used. According to the literature [14], the material parameters of the main body of the pipeline corridor adopt the materials commonly used in the current project, as shown in Table 2, and the soil model parameters are shown in Table 3.

Table 2. Material parameters of pipe gallery model

Structure	Material type	Unit weight (Kg/m3)	Elasticity (MPa)	Poisson's ratio	Standard value for tensile strength (MPa)
Pipe corridor	C40	2500	32 500	0.2	2.39
rebar	HRB400 Φ14/16/20	7860	200 000	0.3	540
prestressing steel strand	Φs15.2 mm (1×7)	7921	195 000	0.3	1860

Table 3. Soil model material parameters

Soil type	Unit weight ($kg \cdot m^{-3}$)	Elasticity (Mpa)	Poisson's ratio	Cohesive (kPa)	Internal friction angle (°)	Porosity ratioe	Permeability ($m \cdot d^{-1}$)
Clay	1900	91	0.3	20	14	0.8	0.06

Reference [15] calculates the precipitation's impact radius. The model can be simplified to a quarter of the model, with pumping wells put in one corner of the model and taking the shape of a quarter of a circle due to the range of the pumping well precipitation impact on the pumping well center as the axis of the center symmetry. More than five times the diameter of the pipe corridor is the impact radius of the excavation of the pipe corridor. The distance from the center axis of the pipe corridor to the pumping well is 30 m, and the width of the soil model is 65 m, considering the effect radius of the pipe corridor excavation and the influence radius of precipitation. The soil model, created using 20 sections of the corridor for examination, has a length of 73.8 m and a height of 30 m. Three meters separate the top plate of the corridor from the ground, while 23.8 meters separate the bottom plate from the soil body's bottom surface. A simplified model of the precipitation conditions is shown in Figure 1.

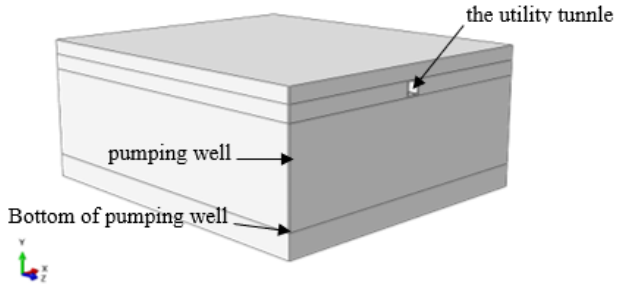

Fig 1. Simplified model of precipitation conditions

2.3. Unit Setup and Contact Setup

The concrete of the corridor is modeled by the concrete damage plasticity model, and the cell is selected as "3D Stress", type C3D8R. The cross-section setting of the steel reinforcement is selected as "Truss" (truss in tension but not in compression), and the mesh cell type is also selected as Truss. The soil is modeled as M-C, and the cell type is C3D8P. The sections are connected by prestressed strands, which are connected to the first and last sections of the corridor by means of Tie constraints in the MPC constraints. The pipe-soil contact and the contact between the pipe sections are made with a "hard" contact in the normal direction and a penalty function with a friction coefficient of 0.3 in the tangential direction [16]. Reinforcing bars are embedded in the pipe joints.

In terms of model boundary condition setting, the normal displacement around the soil body is constrained, and the axial displacement of the first and last pipe corridor is constrained. The pore water pressure of the two cross-sections on the diagonal of the pumping well is calculated according to hydrostatic pressure, and the two sides of the pumping well are symmetric surfaces, and there is no seepage and deformation in the direction on the symmetric surface.

2.4. Model Calculation

Set up two analysis steps. The first step is set to Geostatic, this step is used to balance the soil-ground stress. The second

part is set to soil; this step is used for pore material analysis. In the Geostatic analysis step, kill the corridor unit and calculate the soil unit; in the soil analysis step, kill the soil unit at the pumping well, form the pumping well, kill the soil unit at the corridor, and reactivate the corridor unit to form the corridor model, which can represent the state of the corridor in the case of completed construction. Meanwhile, in this step, use the Keyword command in ABAQUS to set the surface of the pumping well as a free-drainage boundary so that it only drains water to simulate the pumping situation. To ensure continuous precipitation.

3. Model Validation

Before the computations, confirming that the model is reasonable is vital. The parameters of the precipitation test materials are displayed in Table 4, and the specifications of the precipitation model test box are displayed in Figure 2, respectively, according to the literature [17]. The groundwater control soil's initial water level was in a 0.5-m-long area on one side of the box. A mock pit was situated within 0.2 meters of the other side. A simulated pit for pumping wells with two 20-mm-diameter PVC pipes was placed separately in the middle, with a depth of 0.66 m. Water was pumped from the artificial pit using the wells.

The corresponding numerical model was established according to the test setup. The sandy soil was simulated by the M-C model, and the cohesion was taken as the smaller value of 1 kPa. The parameters set for sandy soil hygroscopicity-dehumidification curves in ABAQUS can be selected by combining the parameters of the literature [18–19]. A purely elastic model is used to simulate the glass plate. The numerical model of the test chamber is shown in Figure 3.

Table 4. Material parameters of precipitation test

Soil type	Unit weight ($kg \cdot m^{-3}$)	Elasticity (kPa)	Poisson's ratio	Cohesive (kPa)	Internal friction angle (°)	Porosity ratioe	Permeability ($m \cdot d^{-1}$)
grit	1 700	25×10^3	0.3	1	37	0.69	19.4
glass pane	1 200	$3\ 000\times10^3$	0.2	\	\	\	\

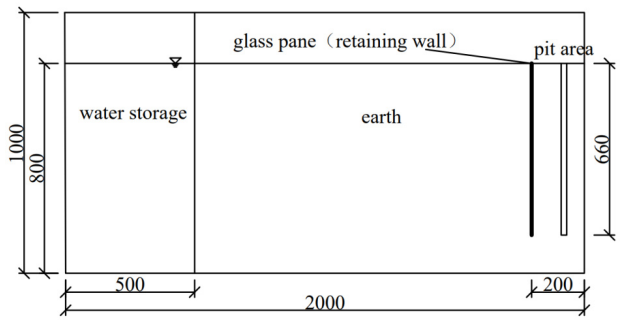

Fig 2. The size of the foundation pit precipitation model test

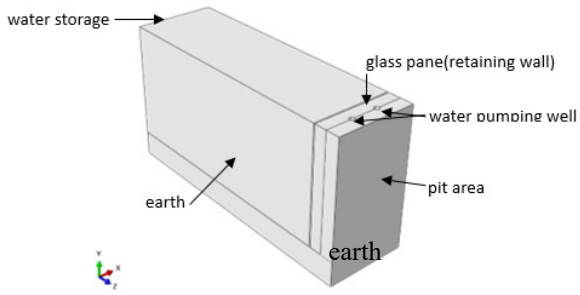

Fig 3. Numerical model of test box

The curves representing the simulated and experimental findings for changes in water level and settlement are shown in Figure 4. The results of the trials and the surface settlement and water level change simulations match, as shown in Fig 4. We may conclude that the model's boundary constraints and precipitation parameters are appropriate and that the simulated settlement outcomes in terms of values and changes in water level are comparable to the real scenario.

4. Simulation Results Analysis

Extracting the surface pore pressure distribution of pumping wells in each condition, the actual precipitation depth with the depth of pumping wells change curve, as shown in Figure 5, the overall performance of the linear relationship, the actual precipitation depth with the pumping wells increase in depth. The actual precipitation depths in each condition are 2.46m, 3.47m, 4.71m, 5.96m and 7.32m from low to high, respectively.

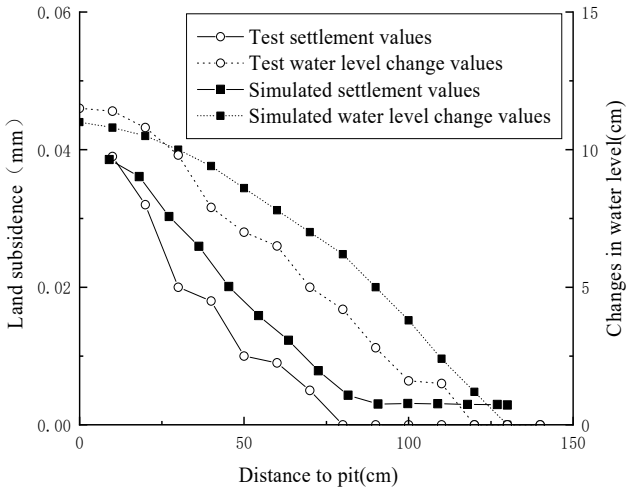

Fig 4. The experimental and simulated values of settlement and water level change

4.1. Actual Precipitation Depth and Soil Settlement under Different Working Conditions

Extract the surface pore pressure distribution of the pumping wells under each condition to get the curve of actual precipitation depth with the depth of the pumping wells, as shown in Fig 5. The overall effectiveness of the linear relationship and the actual precipitation depth with an increase in the depth of the pumping wells. The actual precipitation depths in each situation are 2.46m, 3.47m, 4.71m, 5.96m, and 7.32m from low to high, respectively.

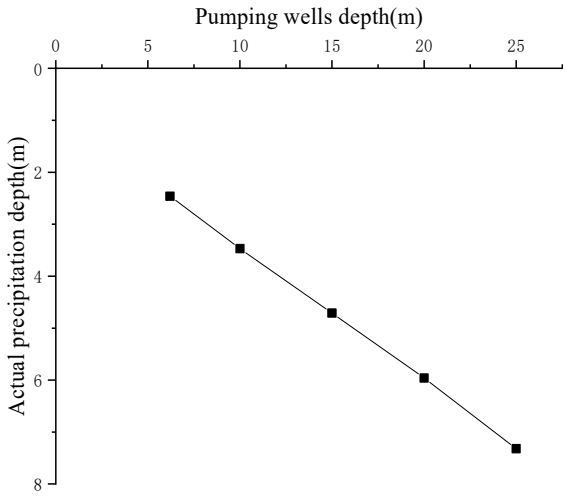

Fig 5. Curve of actual precipitation depth changing with pumping well depth

The surface settlement along the vertical pipe corridor axis changes with distance from the pumping well, as shown in Figure 6, with the vertical axis being the difference between the surface settlement in each condition and the surface settlement without precipitation. From each curve alone, the farther away from the pumping well, the settlement change gradually decreases and then increases when it reaches the location of the pipeline corridor. Taken together, the five curves show that the surface settlement gradually increases as the precipitation depth increases. The maximum settlement changes are all at the nearest point to the pumping well.

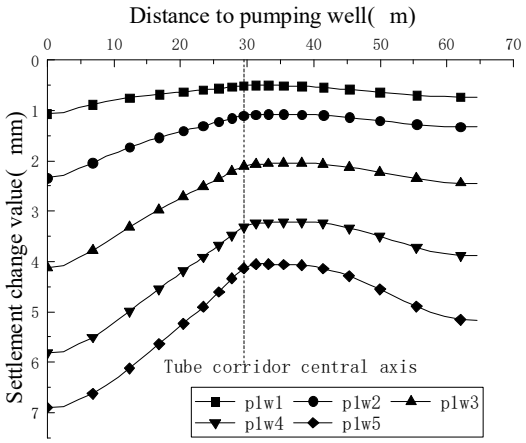

Fig 6. Curve of surface settlement changing with distance from pumping well

The curve of the vertical displacement change value of the bottom plate of the pipe gallery is shown in Fig 7. From the figure, it can be seen that the settlement change gradually slows down as the distance from the pumping well increases. As the depth of precipitation increases, the settlement difference between the first and last ends of the pipe corridor gradually increases, and the settlement change value is also gradually increasing overall.

4.2. Stress Analysis at Mid-Span Location of Top and Bottom Plates on the Outside of the Pipe

Fig. 8 shows the top and bottom plate mid-span stress curves outside the pipe corridor. Both curves display the values for the Mises stress variation.

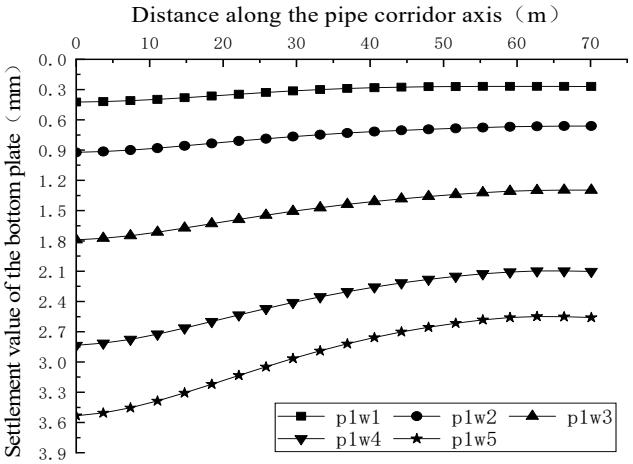

Fig 7. Settlement changes curve of pipe corridor

According to Figures 8(a) and (b), the stress values of the top plate at the spigot joint and the bell joint increase and then fall as the distance together along the pipe gallery's axis increases. The tolerance also gradually rises, with the highest value of each condition rising with the precipitation depth. At the bell joint and spigot joint, the maximum stress variations in the top plate's span are the same. The precipitation depth causes the change's maximum value in bottom plate stress to climb gradually. Under identical precipitation conditions, the junction section of the pipe gallery of sections 1 and 2 displayed the maximum value of the bottom plate's stress change. Since the maximum value of the stress change in the bottom plate span at the socket end is clearly more remarkable than that at the spigot joint, the bottom plate span at the bell junction is weaker and is impacted by the groundwater drop.

Comparing Fig 8 (a) and (c) or Fig. 8 (b) and (d), it can be found that the change of bottom plate force is larger than the change of top plate force on the same port, and the change of bottom plate force can reach 2~3 times the change of top plate force on the interface section near the precipitation point. Therefore, under the precipitation condition, the force change of the bottom plate is larger and more obviously affected.

4.3. Normal Stress at the Joints of the Top and Bottom Plates on the Outside of the Pipe

Reasonable pressure on the interface cross-section is critical for sealing and waterproofing. The change in normal stress at the interface of the top and bottom plates on the outside of the pipe corridor is shown in Fig 9. From Fig 9 (a) and (b), it can be found that the normal stresses at the span center of the top plate are all decreasing and then increasing, and the curves before and after the 30 m are relatively flat, while a clear peak occurs in the working condition p1w5.

From Figure 9 (c) and (d), it can be found that the change rule of normal stress at the bottom plate is opposite to that of the top plate, and the stress change is first increasing and then decreasing, and it becomes 0 at about 20 m. The change in normal stress at the bottom plate at the end of the socket is greater, and it is more obvious to be affected.

Taken together, under precipitation conditions, the normal stress at the mid-span of the top slab gradually decreases in the front section and slightly increases in the back section, and the opposite is true for the bottom slab. The bottom slab has a larger variation and is more significantly affected. The interface section of sections 1 and 2 of the pipe galleries under

the p1w5 condition exhibits the maximum value of change, which is -182.80 kPa. This change has a minimal impact on the assembly pressure of 1.5 MPa in the original interface section and does not cause any harm to the waterproofing and sealing structure of the pipe gallery joints.

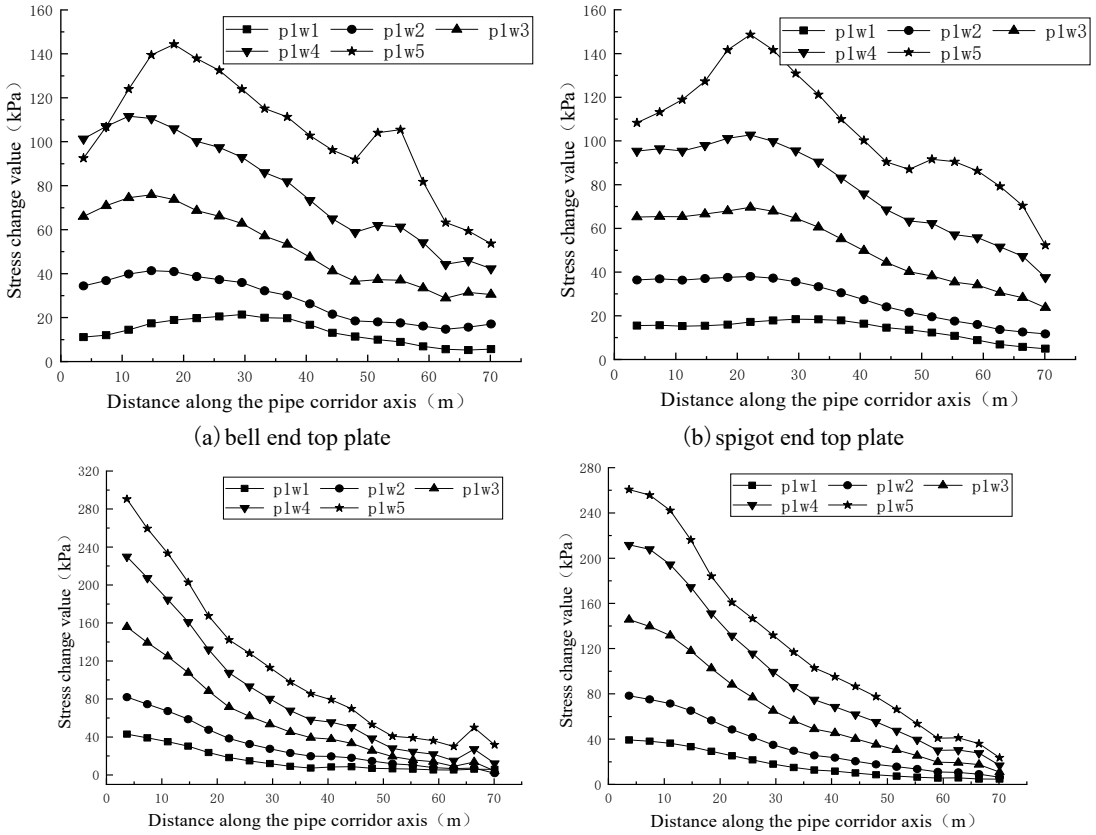

(a) bell end top plate (b) spigot end top plate

(c) bell end bottom plate (d) spigot end bottom plate

Fig 8. Stress curves at the middle of the roof and the bottom plate outside the pipe gallery

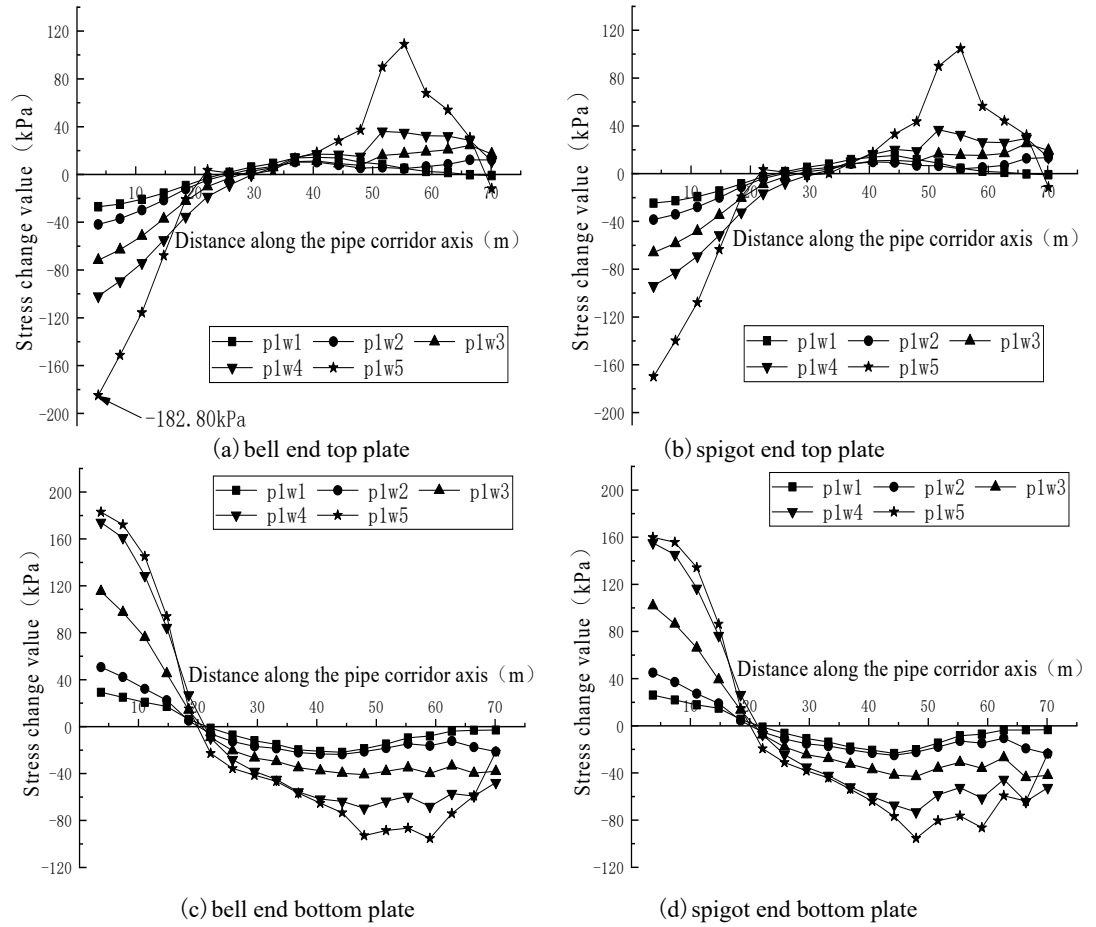

(a) bell end top plate (b) spigot end top plate

(c) bell end bottom plate (d) spigot end bottom plate

Fig 9. Normal stress variation values of the roof and bottom plate outside the pipe gallery

4.4. Stresses at Mid-span Locations of Top and Bottom Plates on the Inside of the Pipe

Under the action of soil pressure, the top plate and bottom plate are bent to the inside of the pipe corridor, and the inner side of the span is the tensile zone. The tensile strength of concrete is obviously lower than the compressive strength, so the stress value of the inner span should be analyzed. The stress curves of the top plate and bottom plate of the inner side of the corridor at the mid-span position are shown in Fig 10, in which the tensile stress change values are shown. Overall, the tensile stresses in the inner top and bottom plates of the pipe corridor are increasing, while the trend of increase decreases with the increase in the distance between the pipe corridor and the pumping well. The magnitude of tensile stresses increases with the depth of precipitation.

The inner tensile stress at the socket end varies more, and the maximum increment of tensile stress is 319.52 kPa at the bottom plate of the socket end in case of p1w5, while the permissible tensile stress of the C40 concrete is 4 MPa. Therefore, the bottom plate of the socket end of the corridor, which is closest to the pumping wells, is at risk of tensile damage in the case of a larger depth of precipitation.

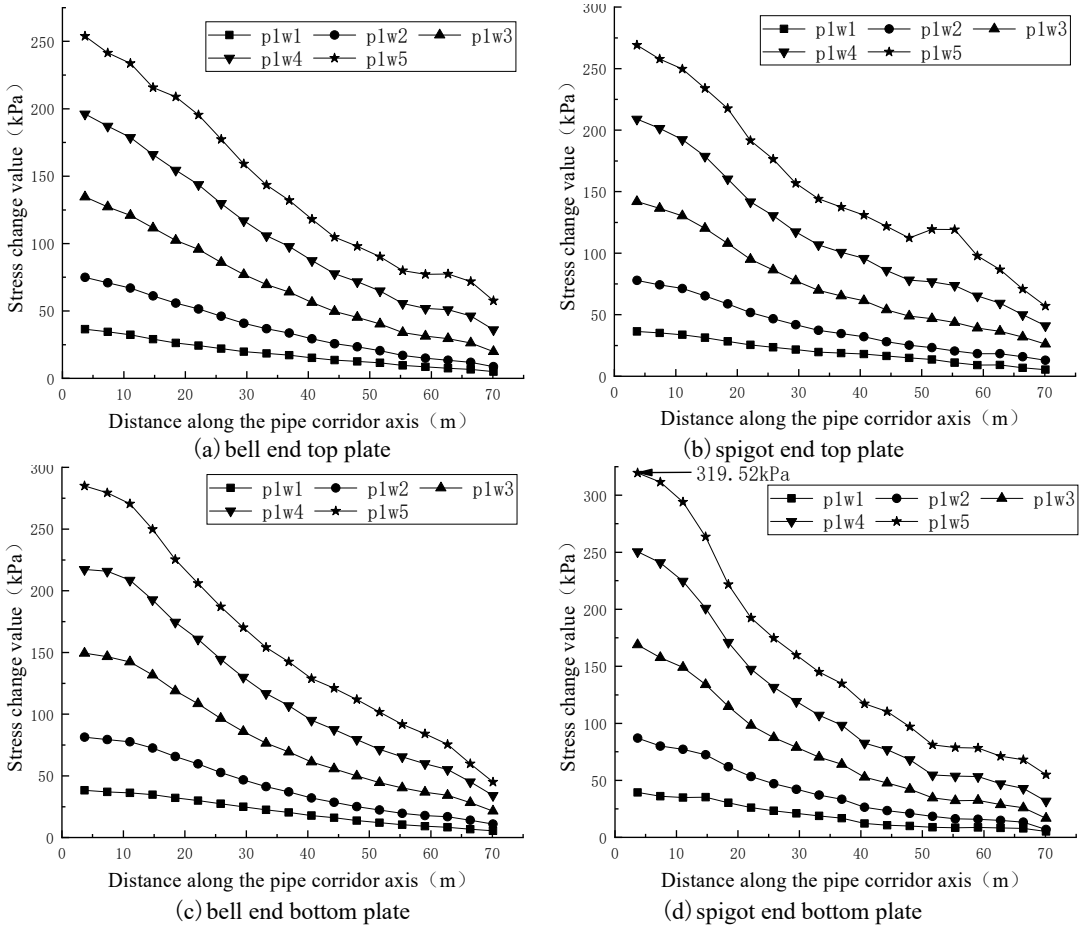

Fig 10. Stress curves at the middle of the roof and the bottom plate on the inside of the pipe gallery

5. Conclusion

In this study, six different types of well-point precipitation working circumstances are built using finite element software, and the corresponding finite element model is created. By comparing the stresses at pipe gallery joints under each working condition, we get the following conclusions:

(1) The force change of the bottom plate on the same port is larger than that of the top plate, and in the interface section close to the precipitation point, the force change of the bottom plate can reach 2~3 times of the force change of the top plate; in the change of the normal stress at the interface, the change of the bottom plate is more obvious, but in the simulated maximum precipitation depth condition, the precipitation work won't damage the sealing and waterproofing structure of the corridor; in the change of the tensile stress at the interface, the maximum tensile stress is 319.52 kPa at the bottom plate at the jack end, and there is a certain risk of damage in tension in the simulation of the maximum precipitation depth condition.

(2) The above results show that the base plate is a part more likely to be involved in engineering accidents during the precipitation work, and in the design and construction, the design and construction testing should be strengthened to check the stress-strain situation of the base plate and to take good water seepage prevention measures for the floor.

(3) The impacts of various precipitation depths on the structural stresses of the corridor are investigated in the study. However, the effects of various precipitation speeds are not considered, and a more thorough investigation of this topic will be carried out in the follow-up work.

Conflict of Interest

The authors acknowledge that they are not affiliated with or associated with any organization or entity that has a financial or non-financial interest in the subject matter or material covered in this manuscript.

References

[1] Curiel-esparza J, Canto-perello J, Calvo MA. (2004) Establishing Sustainable Strategies in Urban Underground Engineering. Science and Engineering Ethics 10(3):523–530.

[2] Canto-perello J, Curiel-esparza J, Calvo V. (2016) Strategic Decision Support System for Utility Tunnel's Planning Applying A'wot Method. Tunnelling and Underground Space Technology Incorporating Trenchless Technology Research 55:146-152.

[3] LEI Shengxiang, Shen Yanjun, Xiao Qinghua, Xi Jiami, Gu Linjun. (2019) Present Situations of Development and Utilization for Underground Space in Cities and New Viewpoints for Future Development. Chinese Journal of Underground Space and Engineering 15(04):965-979. (in Chinese)

[4] Li Xiaojun, Liu Yupeng, Wang Yu. (2017) Recent Achievements and Future Trends for Urban Underground Space Data Standardization. Chinese Journal of Underground Space and Engineering 13(02):287-294. (in Chinese)

[5] Yonglin An, Jin Zhou, Wenxuan Hu, Jiahao Li, (2022) Effect of Water on Tunnel Face and Surrounding Rock Deformation. Indian Geotech J 52, 1–12.

[6] Encarnación Martínez-Moreno, Iván Alhama Manteca, Gonzalo García-Ros. (2019) Network model for the numerical solution of groundwater flow: Application to partially penetrating retaining structures in geotechnical engineering. Computational and Mathematical Methods 1(4):58-67.

[7] P. Gattinoni, L. Scesi. (2017) The groundwater rise in the urban area of Milan (Italy) and its interactions with underground structures and infrastructures. Tunnelling and Underground Space Technology incorporating Trenchless Technology Research 62:167-177.

[8] E Vasilyeva, A Vyaltsev, E Yakovenko. (2019) Safety and Reduction of Technology-Related Risks in the Process of Earth Dams' and Dams' Operation. IOP Conference Series: Earth and Environmental Science 272(2):176-188.

[9] Aswathy, M.S. et al (2020) Prediction of Surface Settlement Due to Deep Excavation in Indo-Gangetic Plain: A Case Study. Indian Geotech J 50, 620–633.

[10] Guangli Xu, Guangda Xu, Shigai Fan, Hongliang Tao, (2015) Impact analysis of groundwater flow changes by underground engineering. Geotechnical Investigation& Surveying 43(01): 41- 44+58. (in Chinese)

[11] Wen Jie Song, Jun Dong, De Hua Liu. (2014) Investigations of Influence of the Variation of Underground Water Levels to the Structural Performance of the Existed Subway Station. Advanced Materials Research 3456:399-404.

[12] J. Mamaghanian, B. V. S. Viswanadham, H. R. Razeghi. (2019) Centrifuge model studies on the performance of geocomposite reinforced soil walls subjected to seepage. Geosynthetics Internationa 1-50.

[13] Maimunah, M. Yeni, D. Kumala. (2019) The Influence of Water Level Fluctuation Reservoir Stability of the Earth Dam. IOP Conference Series: Materials Science and Engineering 506(1):112-124.

[14] Wu Jinglong, Xie Zhongqui, Xu Jian, Jiang Lianzi. (2020) Mechanical properties of single-cabin rectangular vertical prefabricated pipe gallery. Chinese Journal of Applied Mechanics 37(03):1065-1072+1391. (in Chinese)

[15] Li Libing, Hou Xingmin, Li Yuandong. (2021) A finite element method for calculating the influence radius of foundation pit dewatering. Rock and Soil Mechanics 42(02):574-580. (in Chinese)

[16] Wu Jinglong. (2019) Study on the Mechanical Behavior of Underground Comprehensive Pipe Gallery under Heterogeneous Foundation. Changsha, Central South University of Forestry and Technology. (in Chinese)

[17] WANG Pengyu, WANG Shuhong, JIERULA Alipujiang, LIU Weihua. (2018) Umerical Simulation and Analytical Study on Mechanical Behavior of Cast-in-Place Utility Tunnel Joint. Journal of Northeastern University (Natural Science) 39(12):1788-1793. (in Chinese)

[18] Zeng Chaofeng, Wang Shuo, Sone Weiwei, Li Miaokun, Xue Xiuli, Mei Guoxiong. (2021) Control effect of cross walls on metro foundation pit deformation induced by pre-excavation dewatering in soft soils. Chinese Journal of Rock Mechanics and Engineering 40(06):1277-1286. (in Chinese)

[19] Gao You, Sun Dean, Zhang Junran, Luo Ting. (2019) Soil-water characteristics of unsaturated soils considering initial void ratio and hydraulic path. Chinese Journal of Geotechnical Engineering 41(12): 2191-2196. (in Chinese)